JOURNAL OF GEOPHYSICAL RESEARCH, VOL. 106, NO. A8, PAGES 15,643–15,656, AUGUST 1, 2001

Magnetic cloud B_s events and their dependence on cloud parameters

X. P. Zhao and J. T. Hoeksema
W. W. Hansen Experimental Physics Laboratory, Stanford University, Stanford, California

K. Marubashi
Communications Research Laboratory, Tokyo, Japan

Abstract. It had been found that the duration and intensity of the southward interplanetary magnetic field within magnetic clouds (the magnetic cloud B_s event) correlate linearly with the ecliptic latitude of the cloud's central axial field, the one of eight characteristic parameters of expanding magnetic clouds. On the basis of the parameter list determined using the expanding magnetic cloud model for all clouds to be examined, this work examines the dependence of magnetic cloud B_s events on the other seven parameters as well as the ecliptic latitude of the cloud's central axial field. The correlation of the duration and intensity of magnetic cloud B_s events with the ecliptic latitude of the central axial field has been confirmed by the new parameter list with correlation coefficients higher than our earlier study. It is found among the eight parameters that in addition to the ecliptic latitude, the strength of the central axial field, the cloud's bulk speed, and the relative impact distance of the spacecraft to the cloud's central axis are the other parameters that are closely associated with the duration and intensity of magnetic cloud B_s events. There are most probable values for most of the eight parameters of expanding magnetic clouds. In predicting the duration and intensity of magnetic cloud B_s events using the expanding cloud model these most probable values may be used to replace those model parameters that are unavailable from solar observations. This provides a possibility to predict the duration and intensity of magnetic cloud B_s events based on a few parameters that are available from solar observations.

1. Introduction

It is generally believed now that long intervals of large southward interplanetary magnetic field (IMF), B_s events, and the high solar wind speed are the primary cause of intense geospherical disturbances, and the solar source of such geoeffective solar wind structure is the coronal mass ejection (CME) [*Webb et al.*, 2001, and references therein]. However, not all Earth directed fast CMEs are geoeffective, especially during the sunspot maximum phase [*Richardson et al.*, 2000]. Whether or not an Earth directed CME is geoeffective depends on whether or not the CME can produce a B_s event with long duration and strong intensity. Thus understanding the causes of and predicting the duration and intensity of B_s events are a key goal of the space weather research.

There are two kinds of B_s events. One has a solar origin. The solar origin B_s event is actually a part of the internal field of expanding ejecta which are believed to be generated by CMEs and propagate through interplanetary space. The other kind of B_s events originates in the interplanetary space. Most of the interplanetary origin B_s events occur in shock sheaths. Interplanetary origin B_s events are mostly the result of subjecting ambient IMF to the magnetohydrodynamic effects associated with ejecta-stream interactions, stream-stream interactions, or large-amplitude Alfven waves or turbulence in interplanetary space [*Tsurutani and Gonzalez*, 1997 and references therein].

Long-duration strong-intensity B_s events often consist of both the driver gas (fast ejecta) and the shock sheath B_s events [*Tsurutani et al.*, 1988; *Zhao et al.*, 1993]. Nearly every long-duration large-intensity B_s event is associated with ejecta or CMEs. However, the opposite association, the one that is actually useful for storm predictability, is weak; only a fraction of ejecta cause significant B_s events.

Two types of magnetic configuration have been proposed for the internal field of ejecta: the loop-like magnetic tongue [*Gold*, 1962] and the rope-like magnetic cloud (MC) [*Goldstein*, 1983]. The leading polarity of

Paper number 2000JA000421.
0148-0227/01/2000JA000421$09.00

loop-like magnetic tongues has been associated with the global field of their solar source region [*Hoeksema and Zhao,* 1992].

Magnetic clouds (MCs) are defined as a type of ejecta characterized by strong magnetic fields, large rotation in field direction as the cloud moves past a spacecraft, and low proton temperature [*Burlaga et al,* 1981], and have been suggested to be associated with solar origin $\mathbf{B}_s$ events [*Burlaga,* 1991]. It has also been suggested that the field direction on the MC's boundary is consistent with that of the adjacent global magnetic field of the Sun and that the central axial field of MCs is pointed parallel to the inclination of the heliospheric current sheet or coronal streamer belt since the inclination is assumed to be parallel to the orientation of its underlying flux ropes such as filaments and cavities [*Zhao and Hoeksema,* 1996]. The solar cycle evolution of the structure of MCs has shown that it is the overall dipolar magnetic field of the Sun that controls the leading and trailing polarities of MCs, and the orientation of the coronal streamer belt matches the MCs' relative orientation [*Zhang and Burlaga,* 1988; *Bothmer and Rust,* 1997; *Bothmer and Schwenn,* 1998; *Mulligan et al.,* 1998; *Zhao and Webb,* 2000]. In order to quantitatively study the dependence of the duration and intensity of the southward IMF within magnetic clouds (the so-called MCB_s events [*Zhao and Hoeksema,* 1998]) on the orientation of MCs, we have examined the orientation of the central axial field of 26 MCs, determined using the static rope model for 14 clouds [*Lepping et al.,* 1990] and using the expanding rope model for 12 clouds [*Marubashi,* 1997]. It is found [*Zhao and Hoeksema,* 1998] that (1) magnetic cloud central axial field directions can be pointed everywhere between $-90°$ and $90°$ ecliptic latitude; the longitudinal distribution is slightly peaked around the east and west, (2) the duration and intensity of magnetic cloud B_s events correlate with the direction of the cloud's central axial field, and (3) cloud central axial field directions are correlated with the central axial field directions of the associated disappearing filament on the Sun.

In addition to the ecliptic latitude of the MC's central axial field, the MC's bulk speed, the central field strength and the impact distance of the spacecraft to the MCs' central axis, among the eight characteristic parameters of expanding magnetic clouds as shown in the next section, are expected to be associated with the duration and intensity of MCB_s events. This work first determines the characteristic parameters using the expanding rope model for the 11 expanding clouds in Lepping et al. paper. We then figure out the dependence of the duration and intensity of MCB_s events on the eight characteristic parameters of MCs and finally propose a new scheme for predicting the duration and intensity of B_s events on the basis of a few given MC parameters.

2. Characteristic Parameters of Expanding MCs

MCs observed near the Earth are assumed to be a segment of huge loop-like flux ropes whose feet are rooted on the Sun [*Gosling,* 1990] and the magnetic field configuration in MCs can be well described by expanding cylindrical flux ropes [*Osherovich and Burlaga,* 1997]. The magnetic field in an expanding cylindrical flux rope consists of axial and azimuthal components, $B_a$and B_t. These components depend on only the radial distance, ρ, from rope's central axis [*Marubashi,* 1997, and references therein]

$$\mathbf{B} = B_a\mathbf{e_a} + B_t\mathbf{e_t}, \tag{1}$$

$$B_a = B_c J_0(\alpha\rho)(R_0/R)^2, \tag{2}$$

$$B_t = sgn B_c J_1(\alpha\rho)(R_0/R), \tag{3}$$

$$R = R_0(1 + Et), \tag{4}$$

$$v_\rho = \rho E/(1 + Et). \tag{5}$$

Here J_0 and J_1 are Bessel functions of the first kind of order 0 and 1. The field configuration in the rope can thus be characterized by the orientation ($\mathbf{e_a}$) and strength (B_c) of the rope's central axial field, by the handedness (sgn) and intensity (α) of the rope's helicity, and by the rope's expansion rate (E). It is usually assumed that there should be no axial component at the rope's boundary, R. We thus have $\alpha R = 2.404825$ and the helicity intensity α at $t = 0$ can be replaced by the initial radius, R_0, i.e., the radius at the time $t = 0$ when a spacecraft first encounters the rope. It should be noted that the helicity intensity α of expanding clouds weakens as the clouds propagate away from the Sun since the ropes' radius R expands as the time increases. The expansion velocity points radially outward from the central axis. The expansion speed, v_ρ, becomes 0 and the model reduces to the static model when $E = 0$.

The field configuration in MCs observed near the Earth also depends on the radial distance of the spacecraft from the central axis, ρ. In the geocentric solar ecliptic (GSE) coordinate system we have

$$\rho = [(R_0\sqrt{1-p^2} - V_c t\sqrt{\sin^2\theta_c + \cos^2\theta_c \sin^2\phi_c})^2 + (R_0 p)^2]^{\frac{1}{2}}. \tag{6}$$

Here the ecliptic latitude and longitude, θ_c and ϕ_c, indicate the orientation of the central axial field ($\mathbf{e_a}$), V_c the bulk speed of clouds and p, the impact distance relative to R_0, i.e., the shortest distance between the rope's central axis and the line connecting the spacecraft with the Sun.

The eight parameters characterize the magnetic field configuration in expanding magnetic clouds observed by the spacecraft. They are θ_c, ϕ_c, B_c; sgn, R_0 (or α at $t = 0$); and V_c, E, p. The R must be equal to ρ at the

Table 1. Characteristic Parameters of Magnetic Clouds and Magnetic Cloud B_s (MCB_s) Events

Event	Date	Magnetic clouds									MCB_s		Comment
No.	YY:MM:HH	Δt	V_c	R_0	p	E	B_c	θ_c	ϕ_c	sign	I_{bs}	T_{bs}	
		hour	km/s	AU	R_0	hour^{-1}	nT	deg	deg		nT	hour	
M01	65:11:04:13	29	436	0.0812	-0.1537	0.0309598	27.0	33.9	219.9	-1	-7.8	15	
M02	66:11:17:19	18	400	0.0910	0.5329	0.00931966	25.5	75.2	63.2	-1	-9.5	2	
M03	67:01:06:13	19	359	0.0964	-0.5706	0.00199442	18.0	81.1	51.1	1	-0.1	1	
M04	67:05:02:12	26	442	0.1242	0.3097	0.00985222	26.9	-59.4	115.2	1	-24.7	20	
M05	67:12:30:18	39	411	0.1287	0.3885	0.0102987	22.2	-44.3	155.5	1	-14.2	40	
M06	69:02:11:09	33	454	0.1224	-0.3185	0.0178571	20.3	-10.9	238.0	1	-11.4	13	
M07	69:08:26:14	14	407	0.0618	-0.1081	0.00798722	16.7	17.4	289.1	-1	-12.0	7	
M08	71:06:23:10	27	340	0.1007	0.0544	0.00690608	12.0	63.1	100.7	-1	-8.1	5	
M09	73:03:31:23	25	431	0.1223	-0.0401	0.00458926	22.1	-19.0	272.9	-1	-24.7	16	
M10	75:08:01:07	20	368	0.0847	0.6168	0.00605327	18.4	55.6	3.5	-1	-0.5	1	
M11	76:01:10:15	22	382	0.0987	0.2338	0.00434405	21.5	-22.3	271.9	1	-17.6	13	
M12	78:10:30:00	36	385	0.1494	0.0729	0.00533903	14.6	-57.7	110.3	-1	-11.1	25	
L01	67:12:30:18	39	411	0.1287	0.3885	0.0102987	22.2	-44.3	155.5	1	-14.2	40	No. M05
L02	69:02:11:09	33	454	0.1224	-0.3185	0.0178571	20.3	-10.9	238.0	1	-11.4	13	No. M06
L03	71:06:23:10	27	340	0.1007	0.0544	0.00690608	12.0	63.1	100.7	-1	-8.1	5	No. M08
L04	72:11:01:02	18	549	0.0994	0.5064	0.0308642	39.3	9.2	77.5	-1	-22.9	4	
L05	75:11:17:03	27	369	0.1066	-0.4358	0.00335796	15.2	-59.3	20.5	-1	-9.7	15	
L06	78:01:04:19	27	540	0.2855	0.9319	0.00482625	27.5	-1.9	240.2	1	-5.7	4	
L07	78:04:03:18												EMC?
L08	78:06:05:08												EMC?
L09	78:08:27:20	15	443	0.0270	0.4012	0.0202840	31.2	-19.3	350.5	-1	-21.2	16	
L10	78:10:30:00	36	385	0.1494	0.0729	0.00533903	14.6	-57.7	110.3	-1	-11.1	25	No. M12
L11	79:09:18:16	22	369	0.1031	-0.6697	0.00236407	18.6	53.0	161.3	-1	2.8	0	
L12	80:02:16:02	31	379	0.1314	-0.1000	0.00506329	20.3	-31.2	88.9	-1	-14.7	16	
L13	80:03:19:18	41	330	0.1425	0.0723	0.00641026	19.6	5.9	97.2	1	-11.3	19	
L14	80:12:19:12	27	511	0.1133	-0.0019	0.0180832	45.5	-18.9	123.6	-1	-30.0	14	
L15	81:02:07:07	29	452	0.2130	-0.7880	0.00561798	20.0	84.8	344.0	1	2.1	0	
L16	81:03:05:23	24	513	0.0553	0.9409	0.0800000	32.9	29.7	200.6	1	-2.9	1	
L17	82:09:25:20	20	494	0.0818	0.3216	0.0129870	30.0	28.5	139.2	1	-17.7	5	
L18	82:12:20:21												EMC?

time the spacecraft leaves the cloud, the duration of the magnetic cloud is thus not independent of and can be determined by the eight parameters,

$$\Delta t = \frac{2R_0(ER_0 + V_c\sqrt{1-p^2}\sqrt{\sin^2\theta_c + \cos^2\theta_c \sin^2\phi_c})}{{V_c}^2(\sin^2\theta_c + \cos^2\theta_c \sin^2\phi_c) - E^2{R_0}^2}. \tag{7}$$

Table 1 contains two sets of MCs studied by Lepping et al (the lower part) and Marubashi (the upper part). As shown in the last column of Table 1, 4 of Lepping et al' 18 MCs are already in Marubashi's set and 3 MCs seem not to be expanding clouds. Using the expanding rope model, we have determined the eight characteristic parameters for the 11 expanding magnetic clouds in the sample sets of Lepping et al. Table 1 lists the eight characteristic parameters for the 11 expanding clouds as well as the 12 MCs in Marubashi's set. Also included in Table 1 are the observed duration of the B_s part (I_{bs}) and intensity (T_{bs}) of the appropriate MCB_s events. Figure 1 shows histograms for all parameters except the *sgn*. The histograms for the ecliptic latitude and longitude confirm earlier finding that the central axial field of MCs can have basically any orientation, though there are small peaks near the east and west. There are particular values for other five parameters that occur most frequently.

Figure 2 is the scatterplot of the duration and intensity of MCB_s events versus the ecliptic latitude of the 23 MCs' central axil field. The correlation coefficients of the duration and intensity of MCB_s events are -0.78 and 0.64, higher here than -0.74 and 0.52 obtained by the earlier study [*Zhao and Hoeksema*, 1998]. The formulas at the top of panels are the linear regression of the duration and intensity of MCB_s events with the ecliptic latitudes of MCs' central axial field vectors.

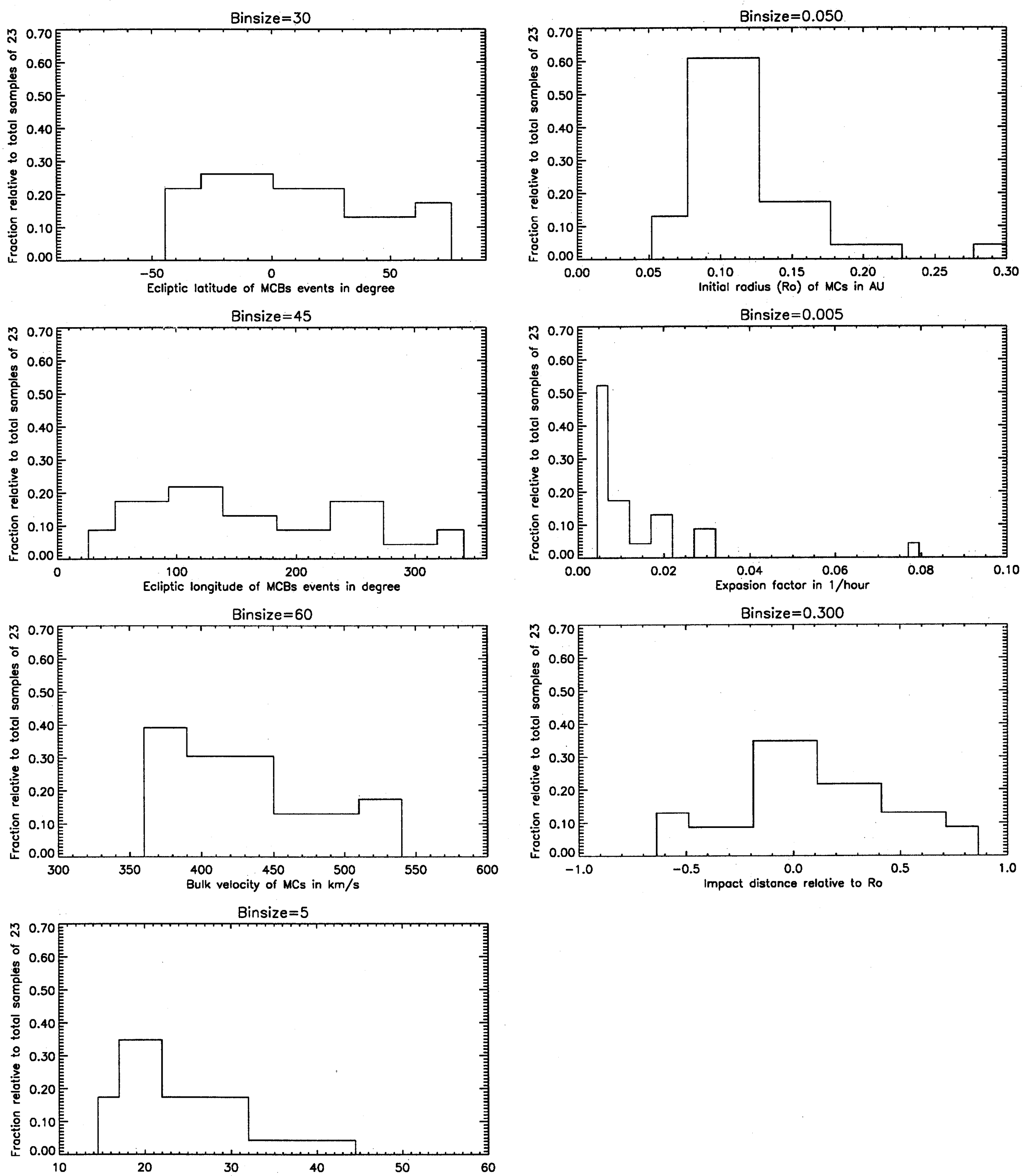

Figure 1. The histograms of seven parameters that characterize magnetic clouds. The parameter is specified at the top of each panel. Also shown on the top is the bin size used to obtain the histograms.

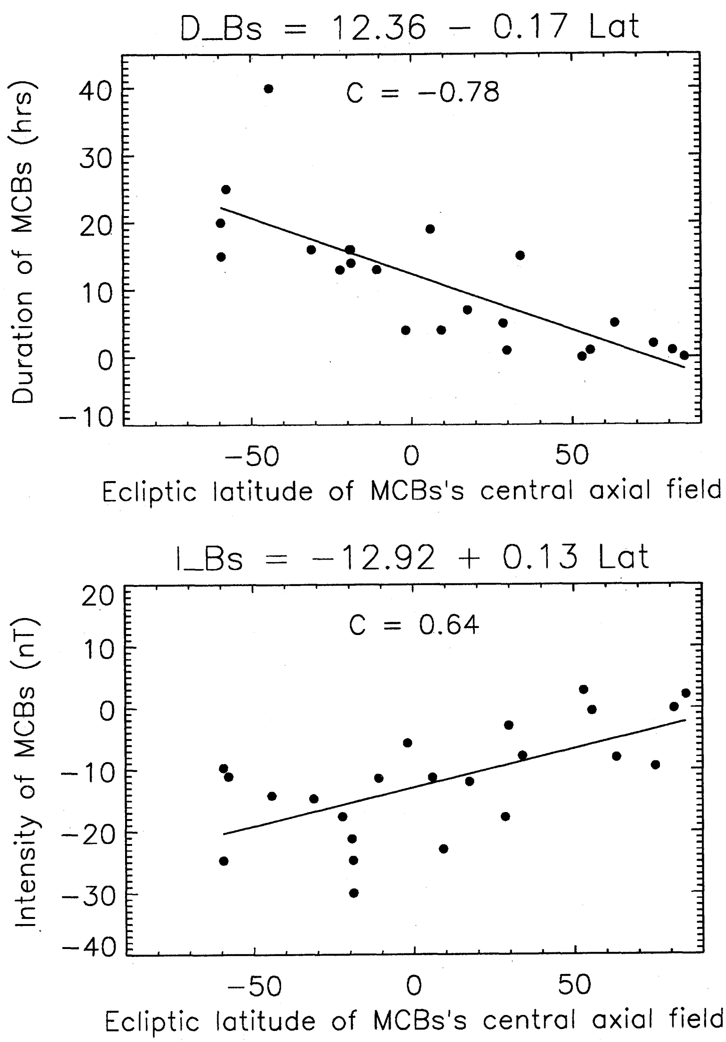

Figure 2. The scatterplots of the duration and intensity of magnetic cloud B_s events versus the ecliptic latitude of the central axial field of magnetic clouds. The formulas on the top of panels are linear regression expression. The values of C denote the correlation coefficients of the duration and intensity with the ecliptic latitude.

3. Modeling MCB_s Events

The north-south IMF component within the 23 MCs in the GSE coordinate system depends on B_a as well as B_t, and can be computed using the eight parameter values in Table 1 using the following formulas:

$$B_z = B_a \sin\theta_c + \frac{B_t \cos\theta_c (\sin\phi_c \cos\beta - \sin\theta_c \cos\phi_c \sin\beta)}{\sqrt{\sin^2\theta_c + \cos^2\theta_c \sin^2\phi_c}} \tag{8}$$

$$\cos\beta = (R_0\sqrt{1-p^2} - V_c t\sqrt{\sin^2\theta_c + \cos^2\theta_c \sin^2\phi_c})/\rho, \tag{9}$$

$$\sin\beta = R_0 p/\rho, \tag{10}$$

where β in (8) – (10) denotes the angle between the direction of $\mathbf{e}_x \times \mathbf{e}_\zeta$ and the azimuthal direction of the rope at the location of the spacecraft. Here $\mathbf{e}_x$ points to the Sun from the Earth and $\mathbf{e}_\zeta$ is the orientation of the rope. Equation (8) shows that only in the case of $\theta_c = 0$, is B_z independent of the axial component B_a.

The solid (dotted) lines in Figure 3 show the computed (observed) bulk speed and magnetic field for magnetic cloud L13 (see Table 1). The two vertical lines indicate the start and end times of the observed cloud. The decreasing speed and the peak in the central axial field strength shifted to earlier times are the characteristics of expanding clouds [(Osherovich et al., 1995]. The shaded area in the bottom panel shows the computed and observed MCB_s event for the cloud; its central axis (θ_c = 5.9° and ϕ_c = 97.2°) is nearly parallel to the ecliptic plane and points nearly to the east. The duration and intensity of MCB_s events discussed below are determined based on the time interval and maximum strength of the southward IMF areas in MCs.

Figure 4 displays computed (solid line) and observed (dotted line) north-south IMF component in the 23 magnetic clouds. The two vertical lines indicate the start and end times of observed clouds. The shaded areas are MCB_s events. The computed MCB_s events

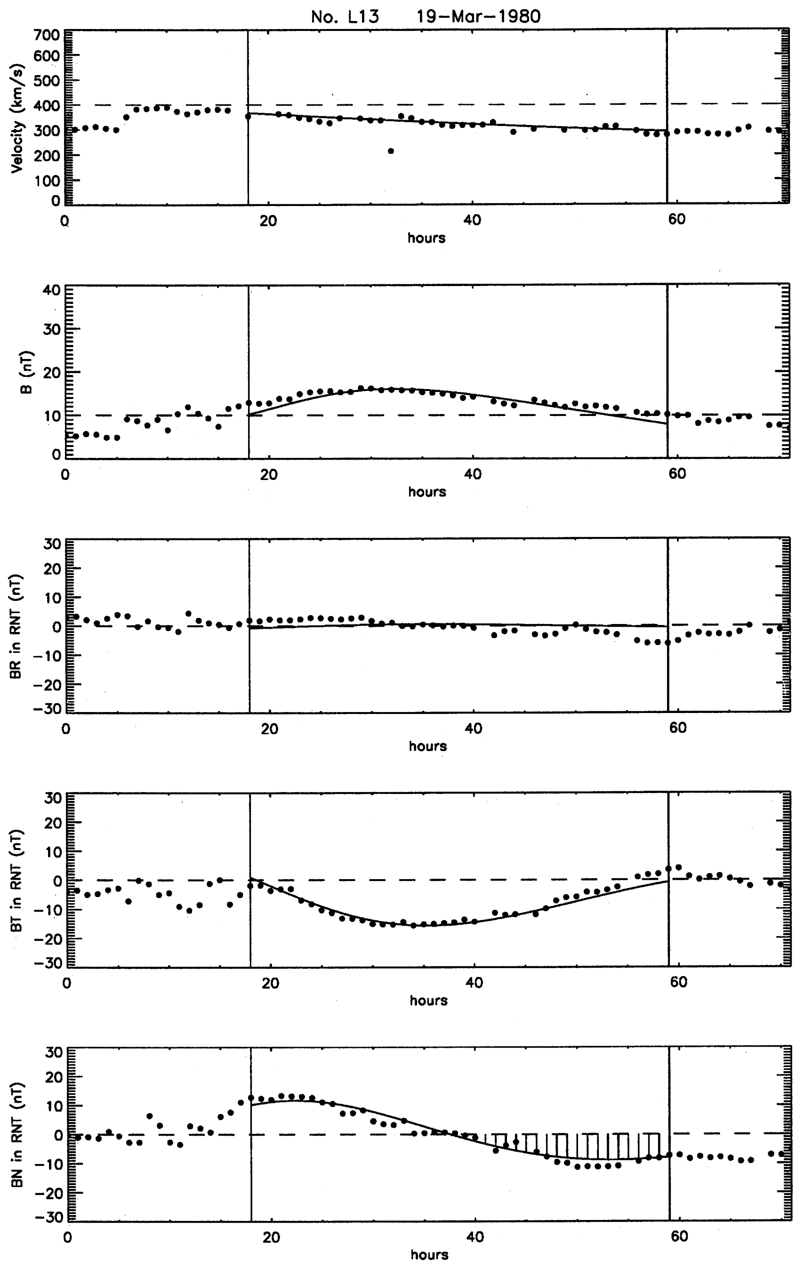

Figure 3. The plasma velocity and magnetic field observed (dotted line) and computed (solid line) for magnetic cloud L13. The shaded area denotes the magnetic cloud B_s event.

agree with the observed ones quite well. The date at the top of each panel is the one when the event was observed. The event numbers shown in panels are consistent with Table 1. The two numbers below the event number are the ecliptic latitude and the longitude. The symbol beside the event number, for example, NWS in the top-left panel, denotes the orientation of clouds used by *Bothmer and Rust* [1997]. Depending on the eight characteristic parameters of MCs, the MCB_s events can have various duration and intensity. Some clouds have no accompanying MCB_s event at all, such as M03 and L11, indicating that not all magnetic clouds can produce B_s events and thus generate magnetic storms. This may explain why many of Earth directed halo CMEs do not generate magnetic storms [*Richardson et al.*, 2000].

4. Dependence of MCB_s Events on MC Parameters

Equation (8) shows that the duration and intensity of MCB_s events depend, in general, on all the eight parameters. However, it is difficult, if not impossible, to obtain all the eight parameters for a MC from solar observations. To predict the characteristics of MCB_s events using fewer parameters, we need large number of events to figure out which of the eight MC parameters most significantly affect the duration and intensity

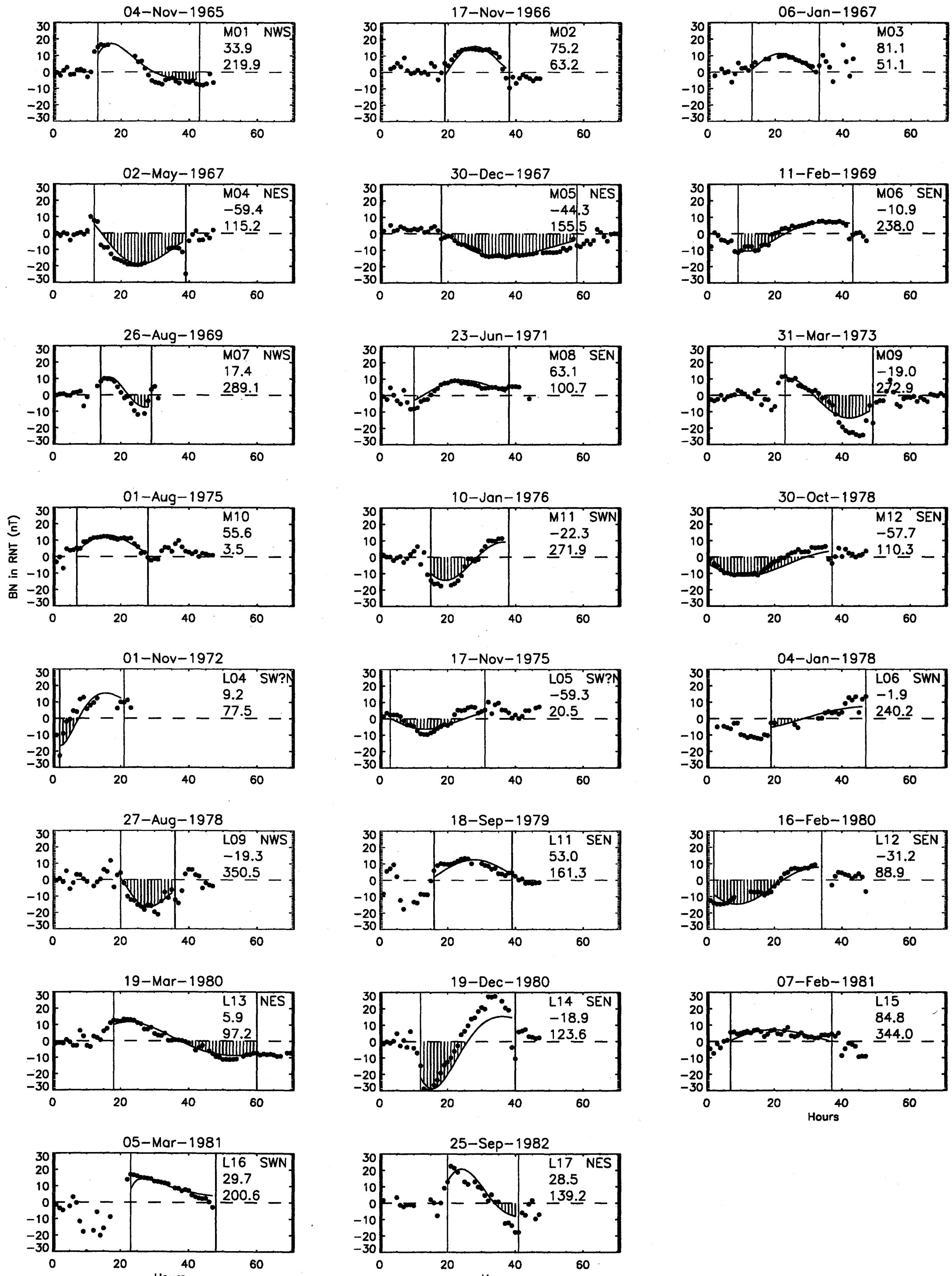

Figure 4. Observed (dotted line) and computed magnetic cloud B_s events for 23 magnetic clouds listed in Table 1. The numbers under the event number are ecliptic latitude and longitude determined by the expanding model.

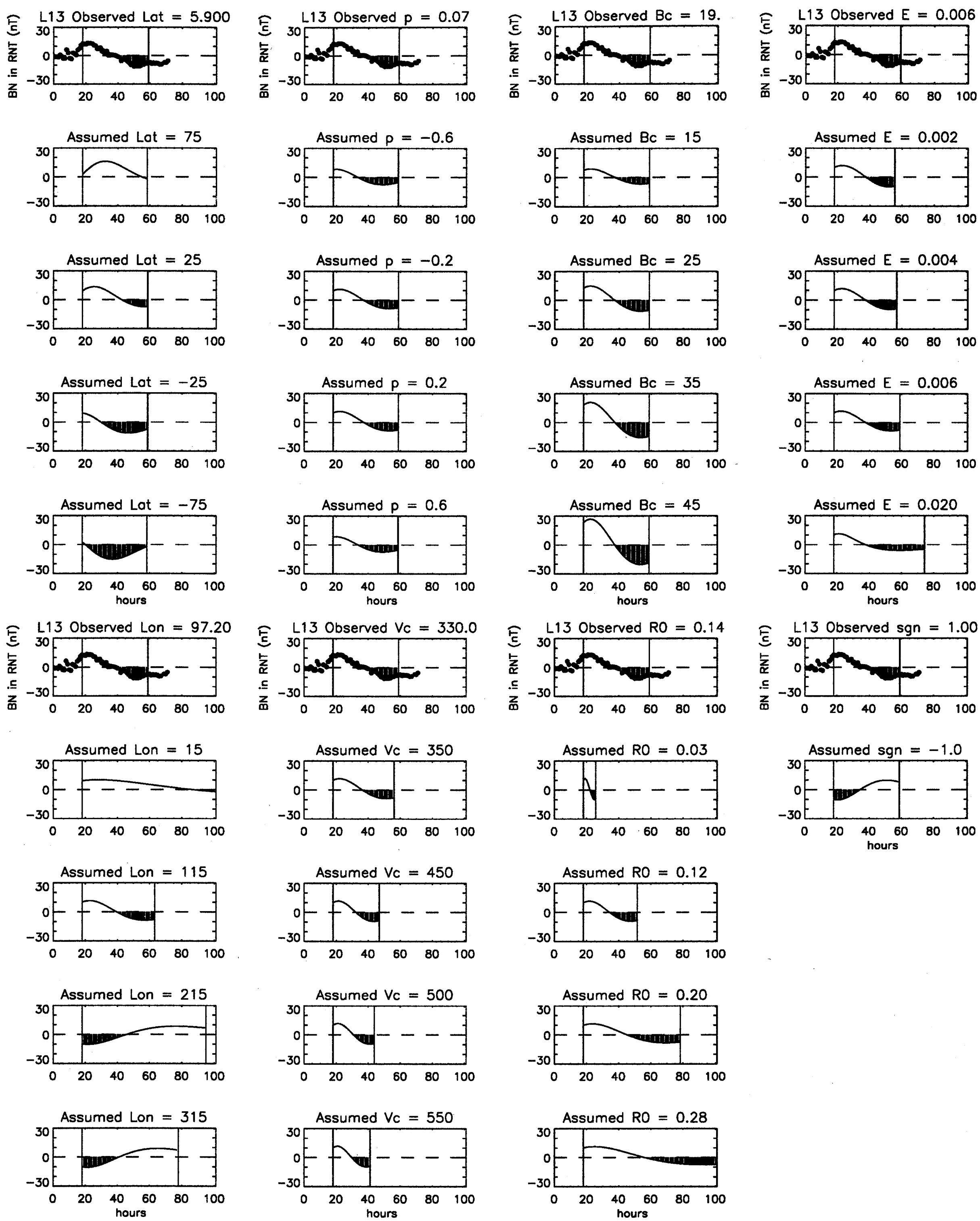

Figure 5a. Simulated magnetic cloud B_s events based on the parameter values in Table 1 for event L13. See text for details.

of MCB_s events. Since the duration of a MC may be determined as well by the eight parameters, many artificial MCs and thus MCB_s events may be obtained using various set of eight parameters as input to the expanding cloud model.

Figure 5a displays 37 panels. Among them, 30 MCB_s events are simulated using (2)–(11) on the basis of Event L13 in which the central axial field vector lies nearly parallel to the ecliptic and point to the east (see Table 1 and Figure 4). The 37 panels are divided into eight subsets according to the eight parameters. Each subset starts with panel labeled "L13" and a specified parameter value on the top of the panel. The dotted line is observed, and the solid line is computed. For example, the solid line in the top panel of the left column is obtained using the specified ecliptic latitude and other seven parameter values for L13 in Table 1. The four panels (only one panel for the "sgn" subset) below the starting panel are obtained by changing the specified parameter while keeping other seven parameters unchanged. For example, the left column contains two subsets; the top one shows the effect of changing ecliptic latitude from 75° to -75° and the bottom one shows the effect of changing longitude from 15° to 315° on the south-north IMF profile. The shaded area in each panel denotes the MCB_s event. The duration and intensity of the MCB_s events can be estimated by the length and the depth of the shaded area.

Figure 5b is obtained with the same parameters as Figure 5a except the parameter sgn is opposite to the

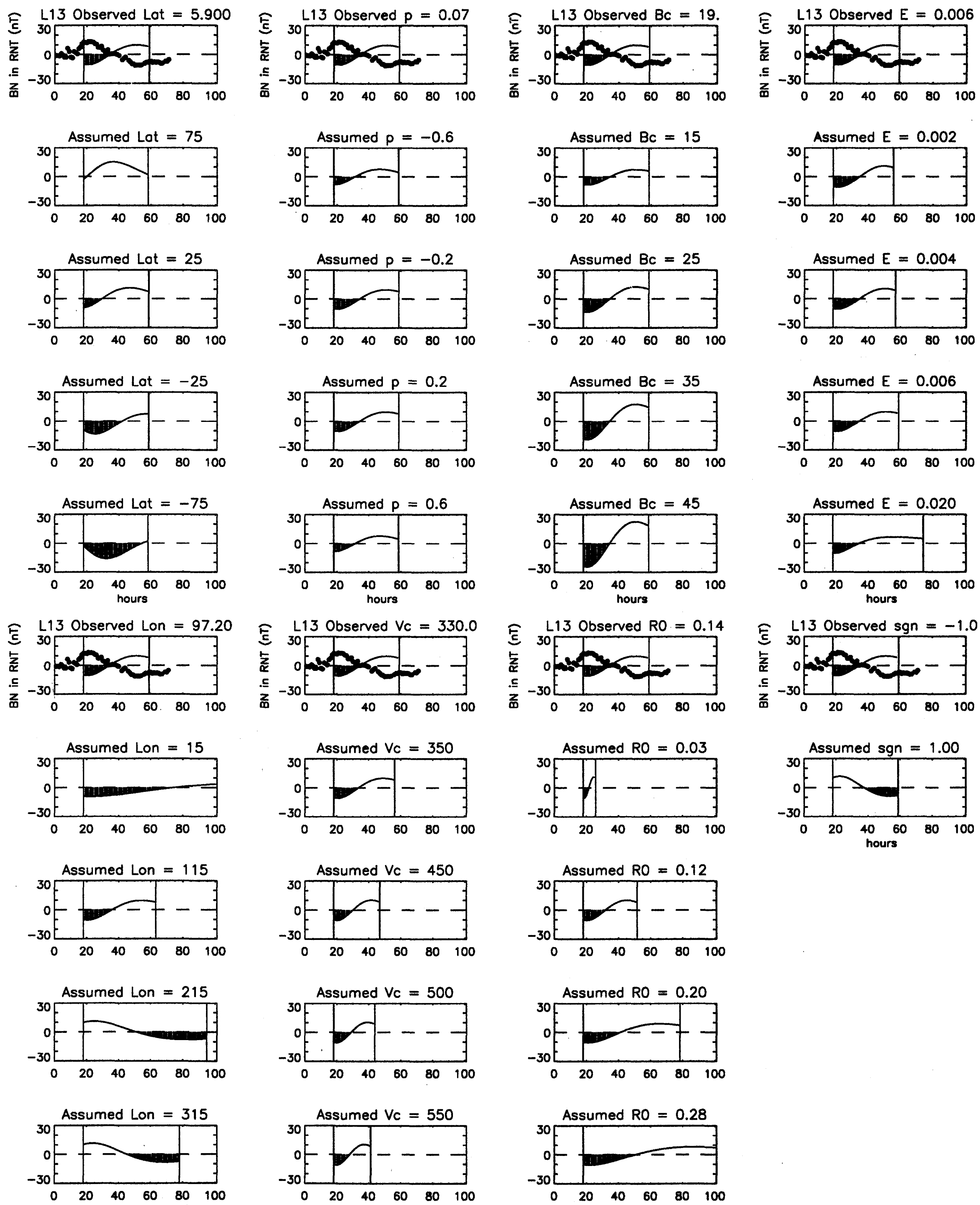

Figure 5b. Same as Figure 5a except the handedness of helicity is opposite

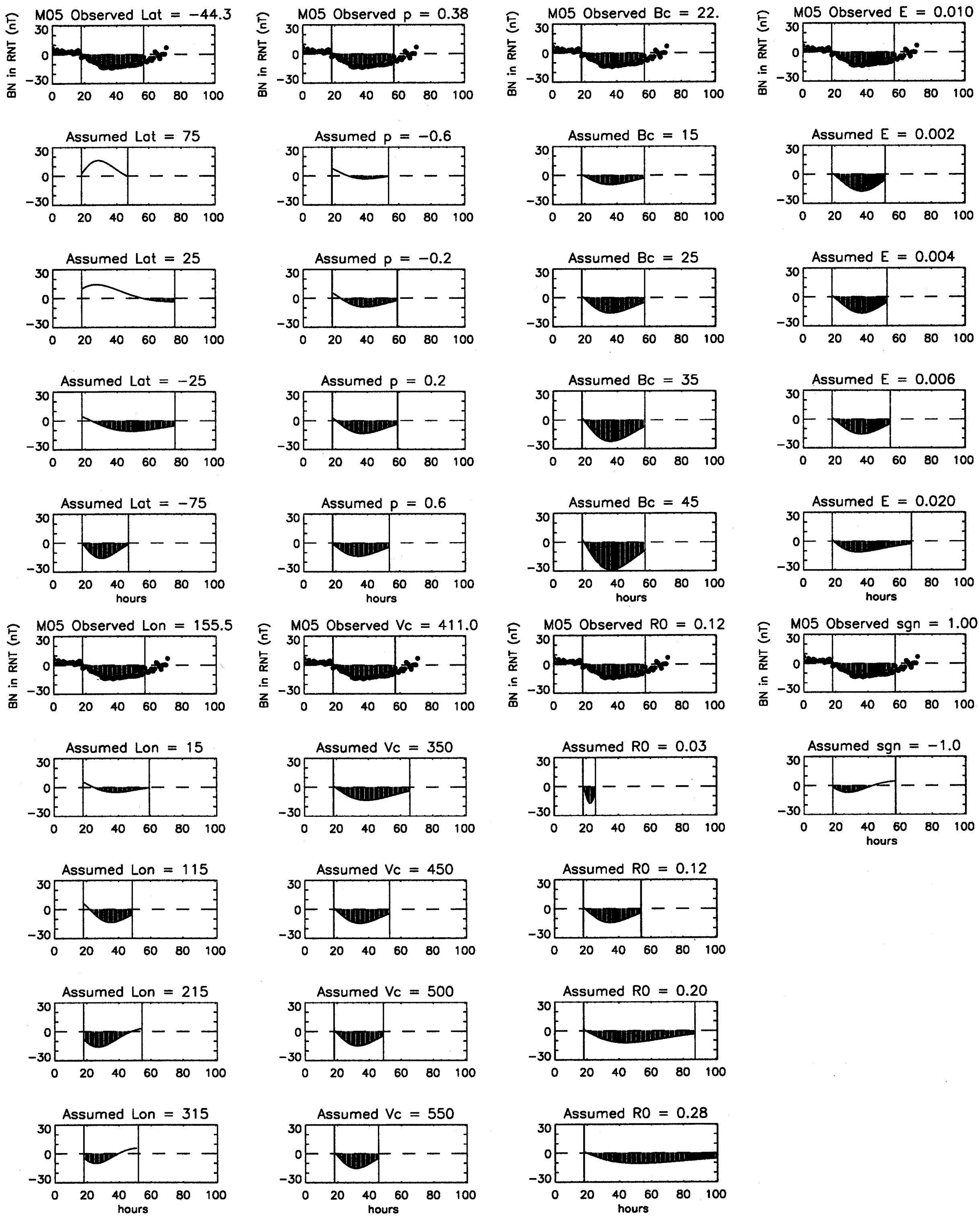

Figure 6a. Simulated magnetic cloud B_s events based on the parameter values in Table 1 for event M04. See text for details.

original sign. It shows the effect of changing the handedness of the helicity on the south-north IMF profile in MCs whose central axial field is nearly parallel to the ecliptic and pointed to the east.

Figures 5a and 5b show that changing the ecliptic latitude of the central axial field vector (Lat) may significantly affect both the duration and the intensity of MCB_s events. The longitude of the central axial field vector (Lon), the bulk speed (V_c), and the initial radius (R_0) may significantly change the duration of MCB_s events, and the central axial field strength (B_c) can affect the intensity of MCB_s events significantly. For MCs with a central axial field vector nearly parallel to the ecliptic, the effect of changing handedness of helicity (sgn), the impact distance (p), and expansion rate (E) is not as significant as the others.

Figure 6a and 6b are obtained based on event M05 (see Table 1 and Figure 4). The ecliptic latitude of the central axial field vector for MC M05 is -44.3°. In addition to the effect mentioned above, the longitude of the central axial field and the impact distance may also significantly affect the intensity of MCB_s events.

5. Prediction of MCB_s Events

Figures 5 and 6 show that the ecliptic latitude of the central axial field vector significantly affect both the du-

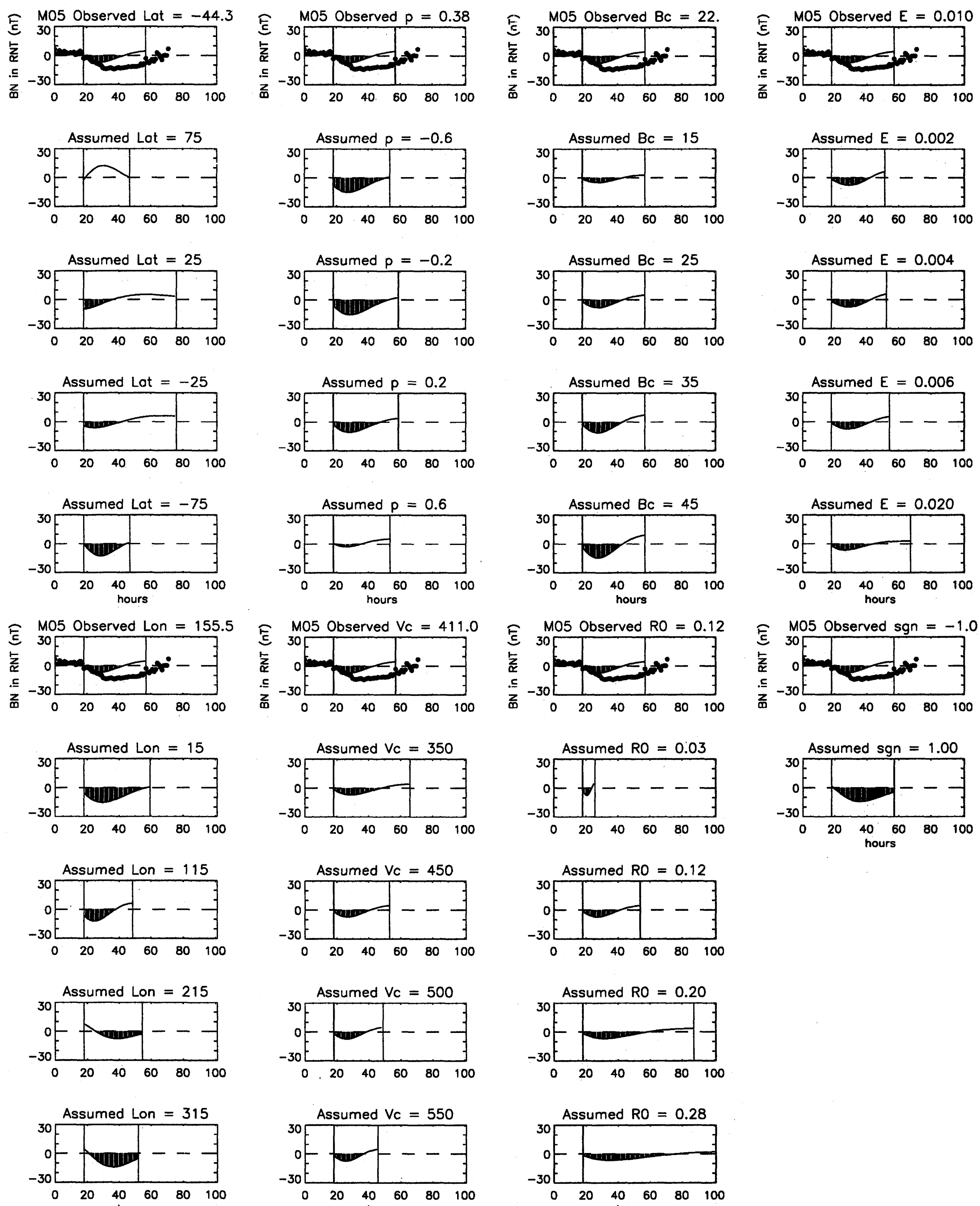

Figure 6b. Same as Figure 6a except the handedness of helicity is opposite

ration and the intensity of MCB_s events. It confirms the finding that there are high correlation coefficients between MCB_s events and the ecliptic latitude. It is also understandable that the central axial field strength and the bulk speed of MCs are major factors for determining, respectively, the intensity and duration of MCB_s events. As indicated in Figure 1, the other parameters have a peak occurrence frequency, i.e., there are most probable values for those parameters. By using these most probable values to replace the unknown values for a specified events we may predict the duration and intensity of an MCB_s event based on the limited available parameter values and (2) – (10).

Figure 7 displays scatter plots of computed duration and intensity versus observed one. The computed duration and intensity in the top two panels are obtained using the linear regression expression on the top of the two panels in Figure 2. The label SIGMA denotes the square root of the average squared deviation of computed from observed duration or intensity,

$$\sigma = \sqrt{\frac{\sum_{i=1}^{n}[X_c(i) - X_o(i)]^2}{n}}. \tag{11}$$

Here X_c and X_o denote computed and observed duration or intensity, $n = 23$. The second row from the top shows the results computed using the values of $\theta_c$in Table 1. The other 7 parameters in (8) are the following: $\phi_c = 115°$, $V_c = 380 \times 3600/1.5 \times 10^8$ AU/hr, $B_c = 20$ nT, $R_0 = 0.1$ AU, $p = -0.1R_0$, $E = 0.005$, and $sgn = -1$ (see Figure 1). The scatter plot in the second row is basically the same as the first row, though the standard deviations in the second row are slightly lower than the first row. The SIGMA in third and the forth rows are continuously decreased as the number of given parameters increases. The SIGMA in the last row is smallest but not zero, suggesting that magnetic clouds are not likely to be perfect cylindrical flux ropes. They may have waves, discontinuities, and likely a noncircular cross section. In addition, the interaction between the ejecta and the ambient magnetic field should also be included in further improving the expanding model.

6. Conclusions and Discussion

For an expanding magnetic cloud observed near the Earth eight parameters are needed to characterize its internal magnetic field configuration and the B_s event within the cloud.

The eight characteristic parameters have been determined using the expanding cylindrical flux rope model for all 23 magnetic clouds examined before. On the basis of the new parameter list the correlation of the duration and intensity of MCB_s events with the ecliptic latitude of the central axial field has been confirmed with the correlation coefficients higher than the coefficients obtained in the earlier study [*Zhao and Hoeksema*, 1998].

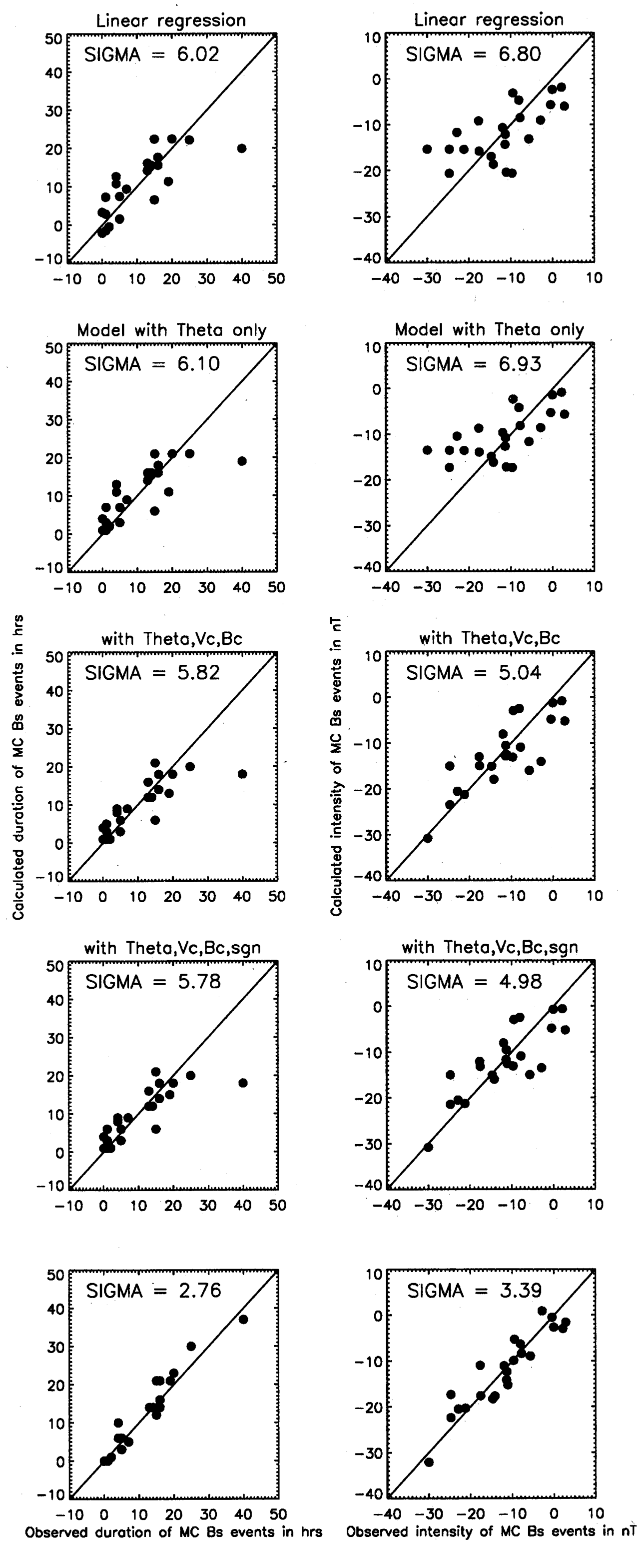

Figure 7. The scatterplots of predicted duration (left panels) and intensity (right panels) versus various given parameters, as shown on the top of each panel. The label SIGMA denotes the square root of the average squared deviation of the computed from observed duration or intensity

Since the duration of a CME is not independent of the eight parameters, many artificial clouds may be created using various sets of eight parameters. These artificial clouds may be used to study the complex dependence of magnetic cloud B_s events on other characteristic parameters of magnetic clouds. It is found that in addition to the ecliptic latitude of MC's central axial field that significantly affect both the duration and intensity of appropriate MCB_s events, the other parameters that significantly affect the MCB_s' intensity are the central axial field strength and relative impact distance, and that significantly affect the MCB_s' duration are the bulk speed, the longitude of the central axial field, and the initial radius.

Some of parameters that are closely related to the MCB_s events may be inferred from solar observations. As shown by recent studies [*Marubashi*, 1986; *Bothmer and Schwenn*, 1994; *Rust*, 1994; *Zhao and Hoeksema*, 1986, 1998; *Elliott et al.*, 2000], the ecliptic latitude of the central axial field may be inferred from observations of solar filaments or from the inclination of the coronal streamer belt or the heliospheric current sheet, though the orientation near 1 AU may be subject to slight change with respect to that near the Sun. The handedness of the flux helicity may be inferred based on the location of the CME source and the hemisphere handedness rule of filaments [*Martin et al.*, 1994]. The bulk speed of magnetic clouds may also be estimated from solar observations [*Gopalswamy et al.*, 2000], though we may expect significant acceleration of initially slow CMEs and deceleration of fast events [*Sheeley et al.*, 1999].

Not all eight parameters are, however, available from solar observations. Fortunately, there are the most probable values for most of the eight parameters. Using the most probable parameter values found in Figure 1 to replace the unavailable parameters, the expanding model may be used to predict the duration and intensity of MCB_s events based on the limited available parameters. The preliminary test shows that the SIGMA for this scheme is smaller than that from the multiple regression. More samples will be tested to see whether or not this method could be used to predict the duration and intensity of MCB_s events and to determine the geoeffectiveness of a CME.

The central axial field strength of coronal mass ejections is important input parameter for predicting the geoeffectiveness of coronal mass ejections. Determining these parameters from solar observations should be one of major goals in the space weather research.

Acknowledgments. This work was supported by the National Aeronautics and Space Administration under grants NAGW 2502 and NAG5-3077, by the Atmospheric Sciences Section of the National Science Foundation under grant ATM9400298, and by the Office of Naval Research under grants N00014-89-J-1024 and N0014-97-1-0129. MDI development was supported by NASA contract NAS5-30386 at Stanford University.

Janet G. Luhmann thanks Rainer Schwenn and Ronald P. Lepping for their assistance in evaluating this paper.

References

Bothmer, V., and D. M. Rust, The field configuration of magnetic clouds and the solar cycle, in *Coronal Mass Ejections, Geophys. Monogr. Ser.*, vol. 99, edited by N. Crooker et al., p. 139, AGU, Washington, D. C., 1997.

Bothmer, V., and R. Schwenn, Eruptive prominences as sources of magnetic clouds in the solar wind, in *Mass Supply and Flows in the Solar Corona*, edited by B. Fleck, G. Noci and G. Polleto, p. 215, Kluwer, Norwell, Mass., 1994.

Bothmer, V., and R. Schwenn, The structure and origin of magnetic clouds in the solar wind, *Ann. Geophys., 16*, 1, 1998.

Burlaga, L. F., Magnetic Clouds, Chapter 5 in *Physica of the Inner Heliosphere, Vol 2*, edited by R. Schwenn and E. Marsch, p. 1, Springer-Verlag, Berlin-Heidelberg, 1991.

Burlaga, L. F., E. Sittler, F. Mariani, and R. Schwenn, Magnetic loop behind an interplanetary shock: Voyager, Helios, and IMP 8 observations, *J. Geophys. Res., 86*, 6673, 1981.

Elliott, D., T. Mulligan, C. T. Russell, and J. T. Gosling, Solar cycle variations in magnetic cloud structure observed by the Pineer Venus Orbiter at 0.7 AU, *Eos Trans. AGU*, 81(19), Spring Meet. Suppl., S364, 2000.

Gold, T., Magnetic storms, *Space Sci. Rev., 1*, 100, 1962.

Goldstein, H., On the field configuration in magnetic clouds, in *Solar Wind Five, NASA Conf. Publ., 2280*, 731, 1983.

Gopalswamy, N., A. Lara, R. P. Lepping, M. L. Kaiser, D. Berdichevsky, and O. C. St. Cyr, Interplanetary acceleration of coronal mass ejections, *Geophys. Res. Lett., 27*, 145, 2000.

Gosling, J. T., Coronal mass ejections and magnetic flux ropes in interplanetary space, in *Physics of Magnetic Flux Ropes, Geophys. Monogr. Ser.*, vol. 58, edited by C. T. Russell, E. R. Priest, and L. C. Lee, p. 343, AGU, Washington, D. C., 1990.

Hoeksema, J. T., and X. P. Zhao, Prediction of magnetic orientation in driver gas associated -B_z events, *J. Geophys. Res., 97*, 3151, 1992.

Lepping, R. P., J. A. Jones, and L. F. Burlaga, Magnetic cloud structure of interplanetary magnetic clouds at 1 AU, *J. Geophys. Res., 95*, 11,957, 1990.

Martin, S. F., R. Bilimoria, and P. W. Tracadas, Magnetic field configurations basic to filament channels and filaments, in *Solar Surface Magnetism*, edited by R. J. Rutten and C. J. Schrijver, p. 308, Kluwer, Norwell, Mass., 1994.

Marubashi, K., Structure of the interplanetary magnetic clouds and their solar origin, *Adv. Space Res.*, 6(9), 335, 1986.

Marubashi, K., Interplanetary magnetic flux ropes and solar filaments, in *Geophysical Monogr. Ser.*, vol. 99, edited by N. U. Crooker, J. A. Joselyn, and J. Feynman, p. 147, AGU, Washington, D. C., 1997.

Mulligan, T., C. T. Russell, and J. G. Luhmann, Solar cycle evolution of the structure of magnetic clouds in the inner heliosphere, *Geophys. Res. Lett., 25*, 2959, 1998.

Osherovich, V. A., and L. F. Burlaga, Magnetic clouds, in *Geophysical Monogr. Ser.*, vol. 99, edited by N. U. Crooker, J. A. Joselyn, and J. Feynman, p. 157, AGU, Washington, D. C., 1997.

Osherovich, V. A., C. J. Farrugia, and L. F. Burlaga, The nonlinear evolution of magnetic flux ropes: 2, Finite beta plasma, *J. Geophys. Res., 100*, 12,307, 1995.

Richardson, I. G., H. V. Cane, and O C St Cyr, Comparison of LASCO Halo CMEs and Ejecta at Earth, *Eos Trans. AGU*, 81(19), Spring Meet. Suppl., S358, 2000.

Rust, D. M., Spawning and shedding helical magnetic fields in the solar atmosphere, *Geophys. Res. Lett.*, *21*, 241, 1994.

Sheeley, N. R., Jr., J. H. Walters, Y.-M. Wang, and R. A. Howard, Continuous tracking of coronal outflows: Two kinds of coronal mass ejections, *J. Geophys. Res.*, *104*, 24,739, 1999.

Tsurutani, B. T. and W. D. Gonzalez, The interplanetary causes of magnetic storms: A review, in *Geophys. Monogr. Ser.*, *98* edited by B. T. Tsurutani, W. D. Gonzalez, Y. Kamide and J. K. Arballo, AGU, Washington, D.C., 77, 1997.

Tsurutani, B. T., W. D. Gonzalez, F. Tang, A.-I. Akasofu, and E. J. Smith, Origin of interplanetary southward magnetic fields responsible for major magnetic storms near solar maximum (1978-1979), *J. Geophys. res.*, *93*, 8519, 1988.

Tsurutani, B. T., W. D. Gonzalez, F. Tang, and Y. T. Lee, Great magnetic storms, *Geophys. Res. Lett.*, *19*, 73, 1992.

Webb, D. F., N. U. Crooker, S. P. Plunkett, and O. C. St. Cyr, The solar source of geoeffective structures, in *Geophysical Monograph Series*, edited by P. Song, G. Siscoe and H. Singer, AGU, Washington, D. C., in press, 2001.

Zhang, G. and L. F. Burlaga, Magnetic clouds, geomagnetic disturbances, and cosmic ray decreases, *J. Geophys. Res.*, *95*, 2511, 1988.

Zhao, X. P. and J. T. Hoeksema, Effect of coronal mass ejections on the structure of the heliospherical current sheet, *J. Geophys. Res.*, *101*, 4825, 1996.

Zhao, X. P., and J. T. Hoeksema, Is the geoeffectiveness of the 6 January 1997 CME predictable from solar observations? *Geophys. Res. Lett.*, *24*, 2965, 1997.

Zhao, X. P., and J. T. Hoeksema, Central axial field direction in magnetic clouds and its relation to southward interplanetary magnetic field events and dependence on disappearing solar filaments, *J. Geophys. Res.*, *103*, 2077, 1998.

Zhao, X. P., and D. F. Webb, Large-scale closed field regions and halo coronal mass ejections, *Eos Trans. AGU*, 81(48), Fall Meet. Suppl., F975, 2000.

Zhao, X. P., J. T. Hoeksema, J. T. Gosling, and J. L. Phillips, Statistics of IMF Bz events, in *Solar-Terrestrial Predictions Workshop–IV*, vol. 2, edited by J. Hruska et al., p. 712, Natl. Oceanic and Atmos. Admini., Boulder, Colo., 1993.

X. P. Zhao, J. T. Hoeksema, and K. Marubashi, W. W. Hansen Experimental Physics Laboratory, Stanford University, Stanford, CA 94305-4085. (xpzhao@solar.stanford.edu)

(Received November 11, 2000; revised April 4, 2001; accepted April 4, 2001.)